PUBLISHED BY THE AMERICAN CHEMICAL SOCIETY

A JOURNAL DEDICATED TO NANOSCIENCE AND NANOTECHNOLOGY

NANO LETTERS

APRIL 2009

VOLUME 9, NUMBER 4 pubs.acs.org/NanoLett

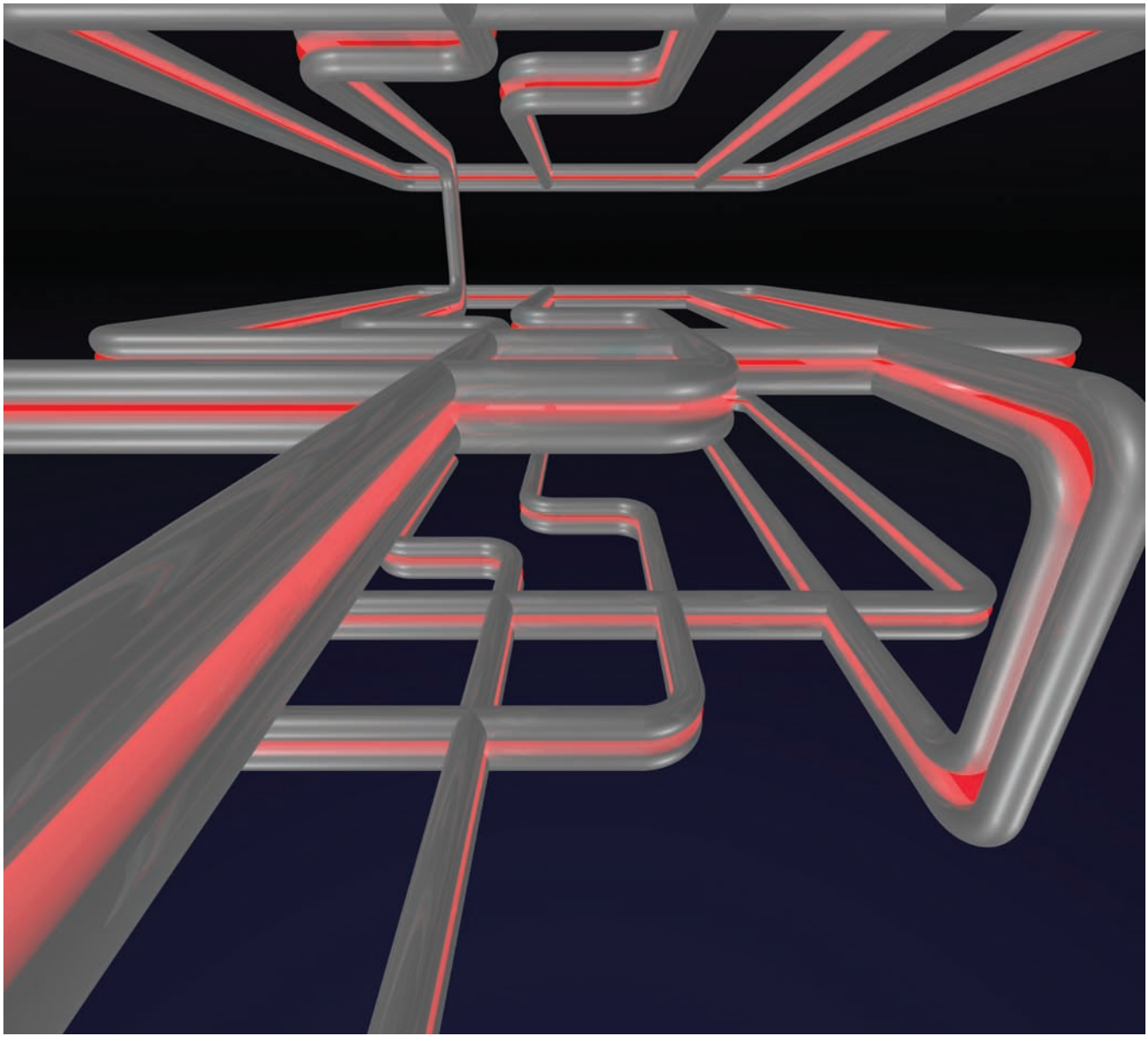

Paired Nanowires Make Robust Plasmonic Waveguides

ACS Publications
High quality. High impact.

www.acs.org

NANO LETTERS

2009
Vol. 9, No. 4
1285-1289

Robust Plasmon Waveguides in Strongly Interacting Nanowire Arrays

A. Manjavacas and F. J. García de Abajo*

Instituto de Óptica—CSIC, Serrano 121, 28006 Madrid, Spain

Received July 10, 2008; Revised Manuscript Received July 18, 2008

ABSTRACT

Arrays of parallel metallic nanowires are shown to provide a tunable, robust, and versatile platform for plasmon interconnects, including high-curvature turns with minimum signal loss. The proposed guiding mechanism relies on gap plasmons existing in the region between adjacent nanowire pairs and multiwire arrays. We focus on square and circular silver nanowires in silica, which we demonstrate to perform much better than previous schemes in terms of a relevant figure of merit measuring the degree of allowed integration. Our work provides the tools for designing plasmon-based interconnects and achieving a high degree of integration with minimum cross talk between adjacent plasmon guides, which should be relevant ingredients for future multiplexed biosensors.

Electromagnetic modes in metal surfaces known as plasmons can propagate along millimeters in metallic structures at near-infrared frequencies,[1] thus providing a plausible substitute for the electrical impulses used in current electronic circuits operating at microwave clock frequencies.[2,3] Several designs of plasmon interconnects have been prototyped in recent years, including metallic waveguides of finite cross section in symmetric[4,5] and asymmetric[6] environments, channels[7] and ridges[8] patterned into flat surfaces, plasmon-band gap structures based upon periodic corrugations,[9] and plasmon hopping in arrays of nanoparticles.[10,11] A promising hybrid system consisting of a dielectric wire positioned close to a silver planar surface has been recently proposed for large optical confinement and long propagation distance.[12] Plasmon waveguides are advantageous over their dielectric counterparts because the metal skin depth makes them highly compact.[5,6] This generates large light intensity concentration, which allows nonlinear optics[13] and sensing[14] applications. Plasmon modes can be tuned in frequency, and their spatial distribution molded, by tailoring the geometry of metallic structures on the nanometer scale, using either direct lithographic methods[15] or chemical synthesis.[16] In particular, extreme plasmon confinement has been achieved in narrow insulator films buried inside metal.[17] Actually, buried structures provide a natural but technologically challenging approach to compact integration. In contrast to that, open plasmonic geometries involve electromagnetic fields extending significantly away from the metal[5−7,9−11] and consequently producing a substantial degree of cross talk between neighboring waveguides.[18]

Here, arrays of parallel metallic nanowires are shown to provide a versatile and tunable platform for highly integrated plasmon interconnects. The propagation distance and degree of confinement of the plasmon guided modes depend strongly on the separation between wires. Individual wire modes are recovered at large separations, while mode hybridization is observed when the spacing is reduced. Gap modes are observed at small separations, highly localized in the regions between two adjacent wires. The dispersion relation of these gap modes is rather insensitive to the number of wires in the structure. We study them by using the boundary element method (BEM)[19] and a two-dimensional multiple-elastic-scattering multipolar expansion of the fields for straight cylinders (2D-MESME),[20] with the two approaches resulting in complete agreement on the scale of the plots. These methods provide rigorous solutions of Maxwell's equations in frequency space for materials described by local dielectric functions and separated by abrupt interfaces. We focus on silver nanowires of circular and square cross sections embedded in silica. The dielectric functions of silver[21] and silica[22] have been taken from optical data. The proposed guiding mechanism is demonstrated to be tolerant to asymmetry in wire pairs and sharp turns of subwavelength radius. The balance between the degree of confinement and the propagation distance is shown to depend critically on geometrical shape and separation, which we study in particular for intermediate cross sections between the circle and the square.

The localized plasmons sustained by our structures can be conveniently characterized using the photonic local density of states (LDOS), defined by analogy to its electronic counterpart as the combined local intensity of all eigenmodes of the system under investigation. We in particular consider the LDOS relative to its value in vacuum, ω^2/π^2c^3. The LDOS is proportional to the radiative decay rate of excited

* Corresponding author, jga@cfmac.csic.es.

10.1021/nl802044t CCC: $40.75
Published on Web 08/02/2008

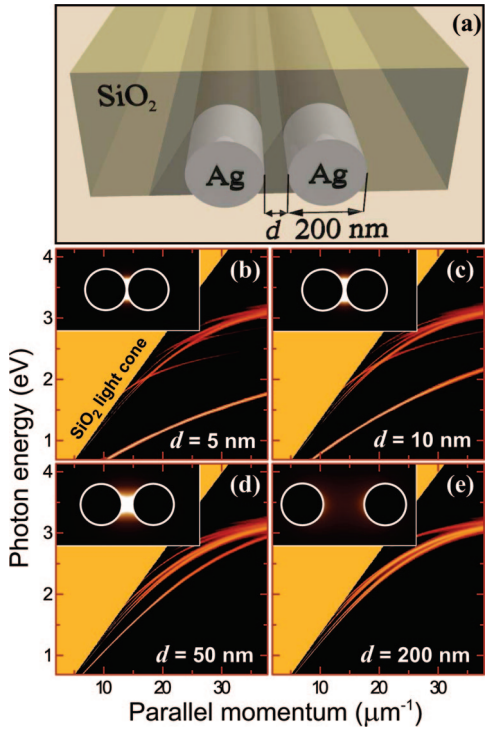

Figure 1. Gap plasmon modes of two parallel silver nanowires in silica. (a) Schematic view of the geometry. (b)−(e) Photonic density of states (DOS) as a function of energy and momentum parallel to the wires for various wire-pair separations d. The insets show the spatial distribution of the local density of states (LDOS) for the lowest-energy gap mode at a free-space light wavelength of 1550 nm. Brighter regions correspond to higher DOS and LDOS. The maximum LDOS in the inset of (c) is ∼15000 times the vacuum value.

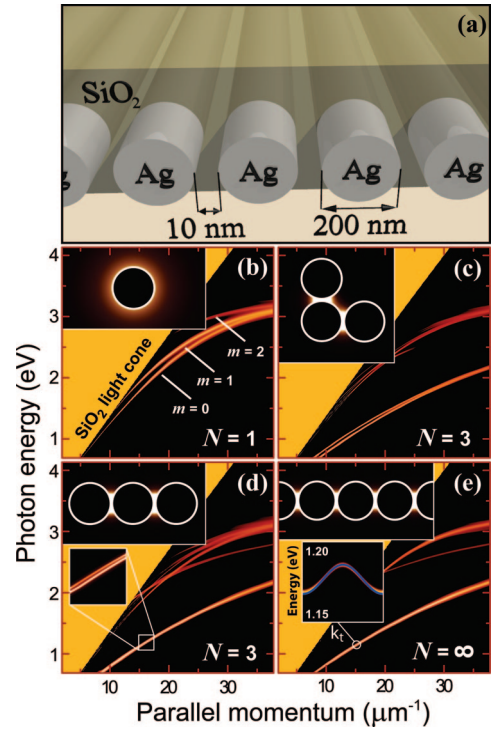

Figure 2. Evolution of gap plasmon modes with the number of nanowires in an array (N). (a) Schematic view of the geometry. (b)−(e) DOS as a function of energy and momentum $k_{||}$ parallel to the wires for arrays of $N = 1$, 3, and ∞ nanowires. The insets show LDOS maps for the lowest-frequency gap mode at a wavelength of 1550 nm. The lower inset in (e) shows the transverse momentum dependence of the DOS for $k_{||} = 16\ \mu m^{-1}$ compared to a tight-binding model of the gap mode (blue solid curve) over the first Brillouin zone of the one-dimensional lattice.

atoms,[23] which we in turn obtain using BEM from the imaginary part of the self-induced electric field acting back on a dipole.[24] We have double checked our results by comparing with the excess of space-integrated total density of states (DOS) with respect to vacuum, which is directly accessible through 2D-MESME.[23]

We start by considering a wire pair formed by two 200 nm circular silver wires embedded in silica, as shown in Figure 1a. The contour plots of Figure 1b−e show the DOS resolved in contributions of different momentum $k_{||}$ parallel to the wires for various separations between wire surfaces (d). A strongly bound mode is observed at small wire separations (Figure 1b), with $k_{||}$ well above k_h, the momentum of light in the host silica. The spatial extension of this gap mode is limited to the interwire region (see inset), and thus, it is expected to interact very weakly with other structures sitting in the vicinity of the wires but far from the gap. This mode evolves continuously for increasing interwire distance to become a hybridized monopole−monopole mode of induced-charge pattern (+)•••(−) within the transversal plane shown in the insets (Figure 1c−d). This is in contrast to the (+−)•••(+−) dipole−dipole plasmon in particle dimers,[25] which is the lowest-energy mode according to plasmon chemistry arguments.[26] In this sense, wires are distinctly different from particles because charge neutrality is guaranteed by oscillations along the rods for finite $k_{||}$, thus making two-dimensional "monopoles" possible in the transverse plane. At sufficiently large separation, single-wire plasmons of $m = 0$ azimuthal symmetry are recovered (cf. Figure 1e and Figure 2b; see ref 27 for analytical expressions of single-wire plasmons).

Figure 2 proves that the gap mode is really local. The lowest-frequency plasmon branch of the three-wire sets in panels c and d of Figure 2 follows approximately the dispersion relation of the gap mode in the wire pair with the same gap distance $d = 10$ nm (Figure 1c), although closer examination reveals the splitting of this mode into two very close modes (see lower inset in Figure 2d). In the infinite wire array of Figure 2e a plasmon branch of gap modes is found for each value of the transverse momentum k_t, parallel to the array plane and perpendicular to the wires ($k_t = 0$ in the figure). All of these branches lie very close to each other, again as a result of weak intergap interaction. Incidentally, propagation across wires mimics plasmon hopping in particle chains.[28]

Three nearly touching wires can be regarded as wire pairs formed by two coupled gaps, and similarly, N-wire arrays behave as structures formed by $N - 1$ gaps. The large degree of plasmon localization observed for small d suggests using a tight-binding model,[29] in which an unperturbed Hamiltonian H_0 describes uncoupled gap modes $|j\rangle$ at sites j, such that $\langle j|H_0|j'\rangle = \omega_{k_{||}}\delta_{jj'}$, where $\omega_{k_{||}}$ is the mode energy for fixed $k_{||}$.

Neighboring gaps can interact in this model via a potential V, with nonzero matrix elements $\langle j|V|j \pm 1\rangle = \Delta_{k_\parallel}/2$, where $\Delta_{k_\parallel}$ is the hopping energy. Then, the two modes of the linear three-wire set have energies $\omega_{k_\parallel} \pm \Delta_{k_\parallel}/2$ (i.e., the wire-pair band lies halfway between the two three-wire-set bands, which we have verified by comparison of Figures 1c and 2d). Also, the plasmon modes of an infinite, periodic wire array must have the form $|\psi_{k_t}\rangle = \sum_j \exp(ik_t aj)|j\rangle$ by virtue of Bloch's theorem,[29] where a is the period. These states diagonalize the full Hamiltonian $H_0 + V$ and have energies $\omega_{k_\parallel k_t} = \omega_{k_\parallel} + \Delta_{k_\parallel}\cos(k_t a)$. We have tested this formula in the array of Figure 2e, where the lower inset shows $\omega_{k_\parallel k_t}$ as a function of k_t for $k_\parallel = 16\ \mu m^{-1}$ (solid curve) compared with the actual 2D-MESME calculation of the DOS. The unperturbed gap energy $\omega_{k_\parallel} = 1.18$ eV and the hopping parameter $\Delta_{k_\parallel} = 0.01$ eV have been taken from the wire pair (Figure 1c) and three-wire set (Figure 2d) with the same value of d, respectively. Similar agreement between model and full calculations is observed over the range of $k_\parallel$ under consideration.

Interestingly, these analytical expressions apply to the large d limit as well, in which the tight-binding model is constructed based upon localized plasmons of the wires, showing similar agreement with rigorous DOS calculations. Tight-binding is thus the natural description of both the small and the large d limits in the noted continuous evolution from the localized gap mode (small d) to the lowest-energy hybridized (monopole−monopole) wire modes (large d).[25]

The degree of plasmon localization increases with decreasing gap distance d. This is reflected in a reduction of the phase velocity $v_p = c_h k_h/k_\parallel$ relative to the speed of light in silica, c_h, as shown in Figure 3a. The group velocity (not shown) is also reduced, so that gap modes become considerably slower than light in silica. The propagation distance is strongly dependent on interwire distance (Figure 3b): the large confinement observed at small separations increases the relative weight of the electric field intensity inside the metal, where Ohmic losses are produced in proportion to that intensity within linear response. Nevertheless, the gap mode involves electric field polarization mainly perpendicular to the wire surfaces near the gap, where light energy is concentrated, and this is beneficial to obtain longer propagation distances because the normal electric field inside the metal is reduced by its large dielectric function to fulfill the continuity of the normal electric displacement. This gives rise to propagation distances of the order of tens of micrometers for separations of tens of nanometers, accompanied by relatively large mode confinement. The tradeoff between confinement and propagation distance is clearly illustrated in the long d behavior of the infinite array for $k_t = 0$ and $k_t = \pi/a$, with the former showing longer propagation and larger phase velocity (see Figure 3).

We find it convenient to define a figure of merit F for the waveguides expressed as the ratio between the propagation distance and the geometric mean of the mode diameter in the transverse directions. The quantities F^2 and F^3 should be roughly proportional to the number of logical elements

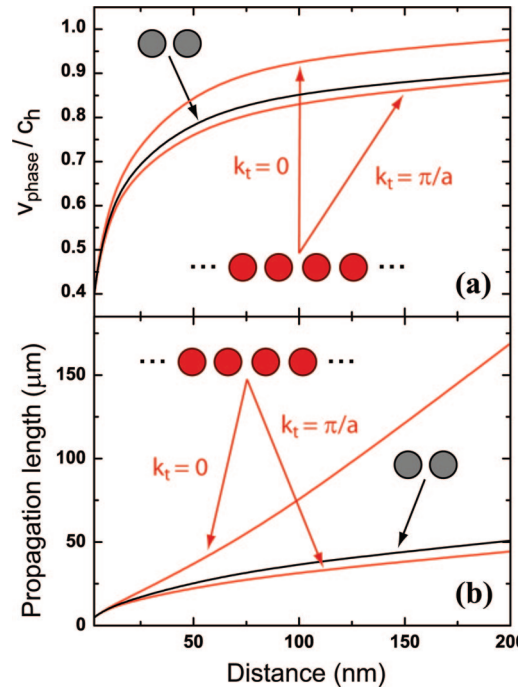

Figure 3. (a) Phase velocity of gap plasmon modes in silver wire pairs and infinite arrays (for $k_t = 0$ and $k_t = \pi/a$, where a is the period) as a function of separation d for fixed wavelength $\lambda = 1550$ nm. (b) Propagation length L under the same conditions as in (a), obtained from $L = 1/2Im\{k_\parallel\}$, where $Im\{k_\parallel\}$ corresponds to the HWHM of the $k_\parallel$-dependent DOS.

that can be integrated using a given waveguiding scheme with two- and three-dimensional packing, respectively. We obtain $F \approx 540$ for the wire pair of Figure 3 at a separation of 10 nm. This has to be compared with values of $F \lesssim 50$ for channel plasmon polaritons[7] and particle arrays,[11] and $F \approx 100$ at 1550 nm in ridge structures.[8] High values of $F \approx 500$ can also be achieved with dielectric wires near silver,[12] specifically designed for planar structures. We conclude that the wire arrays here proposed yield high values of $F \approx 540$, also improved with respect to those obtained for single wires (e.g., $F \approx 100$ at 100 nm radius and 1550 nm wavelength), compatible with high integration of plasmonic circuits. The decrease in propagation length is the price to pay for plasmon confinement, but wire arrays seem to perform optimally with respect to the figure of merit F for 3D-integrable structures.

Reliable plasmon waveguides must be robust against fabrication imperfections and sharp turns. Next, we show that gap waveguides satisfy these requirements. In particular, curved waveguide paths produce radiative losses originating in coupling to propagating light waves when translational invariance is broken. We analyze this effect in Figure 4 both for nonidentical coplanar tori and for identical coaxial tori, using the prescription $k_\parallel = m/b$ to compare with straight waveguide modes, where b is the toroidal radius (see insets) and m is the azimuthal momentum number. The calculations are performed using BEM, specialized for axially symmetric geometries.[19] Radiative losses are still small compared to absorption for $b = 750$ nm (cf. curves for straight wires and large-radius tori in Figure 4, showing only ~3% increase in peak width of curved vs straight wires due to radiative losses

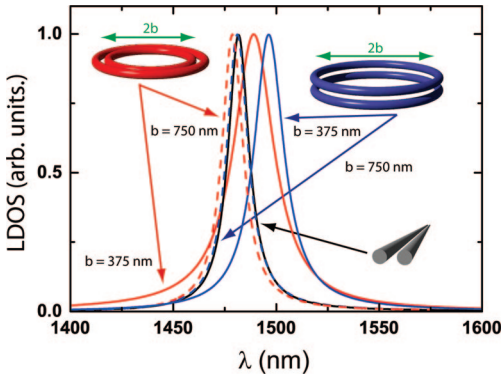

Figure 4. Gap mode in coplanar and coaxial bitori compared with a straight-wire pair for a gap distance $d = 10$ nm. Partial contributions to the LDOS are shown as a function of wavelength for a point in the center of the gap, both at fixed azimuthal number in tori ($m = 8$ for radius $b = 750$ nm and $m = 4$ for $b = 375$ nm) and at fixed parallel momentum in the straight-wire pair ($k_{||} \approx 10.7$ μm^{-1}, such that $k_{||} = m/b$). The curves are normalized to their maximum value.

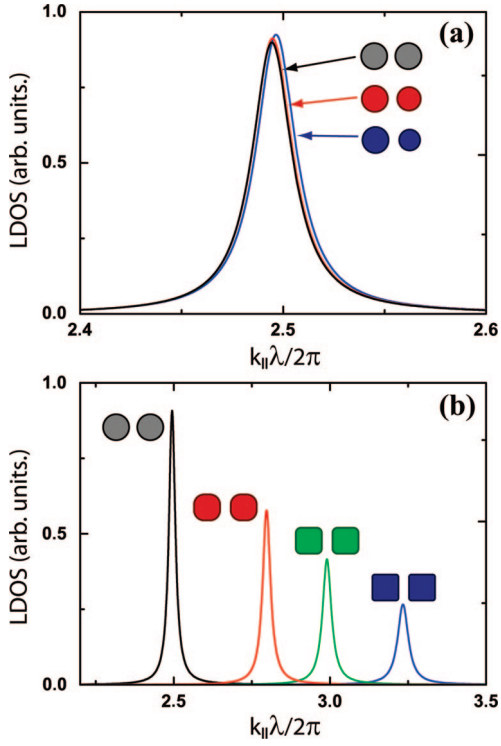

Figure 5. Gap mode against variations of wire radius (a) and shape (from circular to square cross section) (b). The LDOS is represented as a function of $k_{||}$ for a point at the center of each wire pair and a wavelength $\lambda = 1550$ nm. One of the wires in the pairs of (a) has a fixed radius of 100 nm, while various values of the radius are considered for the neighboring wire: 100 nm, 90 nm, and 80 nm, from top to bottom. The distance between wires is $d = 10$ nm in all cases. The horizontal diameter of the wires in (b) is 200 nm for all cross sections.

in the former), but they become sizable for shaper turns (the width increases by 42% and 95% for $b = 375$ nm in coaxial and coplanar tori, respectively).

Guided gap plasmons are also robust against wire-pair asymmetries, as shown in Figure 5a for fixed wavelength $\lambda = 1550$ nm and gap distance $d = 10$ nm. Variations of up to 20% in the relative radius of neighboring wires produce just a small, tolerable shift in $k_{||}$. However, wire shape is a critical parameter, which we study in Figure 5b through the transition from circular to square cross section. This produces a shift of the gap plasmon toward larger $k_{||}$, consistent with the higher degree of confinement that occurs when evolving from the linelike contact of the circular wires to the planar waveguide defined by the square wires, the guided modes of which have been the subject of recent experimental investigation.[17] This increase in confinement is accompanied by peak broadening originating in larger overlap of the gap mode with the metal (Ohmic losses). The observed extreme sensitivity to shape and separation of the wires imposes severe limits to the precision required in the fabrication of the arrays in order to maintain a homogeneous mode wavelength along the waveguide.

In conclusion, we have shown that gap plasmon modes existing in the region defined by two neighboring nanowires are excellent candidates to guide signals over tens of micrometers at near-infrared frequencies. These modes are quite robust against both unintended variations of wire cross section and curvature in short turns, and thus, gap plasmons can be guided with minimum losses over complicated winding paths of micrometer dimensions. Furthermore, gap modes are highly confined to the gap region, so that intermixing between neighboring wire-pairs can be minimized, thus preventing waveguide cross talk and allowing highly integrated plasmonic circuits in three-dimensional spaces.

Acknowledgment. We thank Rebecca Sainidou for useful discussions. This work was supported by the Spanish MEC (MAT2007-66050 and *consolider* NanoLight.es) and by the EU-FP6 (NMP4-2006-016881 "SPANS").

References

(1) Sarid, D. *Phys. Rev. Lett.* **1981**, *47*, 1927–1930.
(2) Ozbay, E. *Science* **2006**, *311*, 189–193.
(3) Zia, R.; Schuller, J. A.; Chandran, A.; Brongersma, M. L. *Mater. Today* **2006**, *9*, 20–27.
(4) Takahara, J.; Yamagishi, S.; Taki, H.; Morimoto, A.; Kobayashi, T. *Opt. Lett.* **1997**, *22*, 475–477.
(5) Berini, P. *Phys. Rev. B* **2000**, *61*, 10484–10503.
(6) Berini, P. *Phys. Rev. B* **2001**, *63*, 125417.
(7) Bozhevolnyi, S. I.; Volkov, V. S.; Devaux, E.; Laluet, J. Y.; Ebbesen, T. W. *Nature* **2006**, *440*, 508–511.
(8) Moreno, E.; Rodrigo, S. G.; Bozhevolnyi, S. I.; Martín-Moreno, L.; García-Vidal, F. J. *Phys. Rev. Lett.* **2008**, *100*, 023901.
(9) Bozhevolnyi, S. I.; Erland, J.; Leosson, K.; Skovgaard, P. M. W.; Hvam, J. M. *Phys. Rev. Lett.* **2001**, *86*, 3008–3011.
(10) Krenn, J. R.; Dereux, A.; Weeber, J. C.; Bourillot, E.; Lacroute, Y.; Goudonnet, J. P.; Schider, G.; Gotschy, W.; Leitner, A.; Aussenegg, F. R.; Girard, C. *Phys. Rev. Lett.* **1999**, *82*, 2590–2593.
(11) Maier, S. A.; Kik, P. G.; Atwater, H. A.; Meltzer, S.; Harel, E.; Koel, B. E.; Requicha, A. A. G. *Nat. Mater.* **2003**, *2*, 229–232.
(12) Oulton, R. F.; Sorger; V. J.; Genov, D. A.; Pile, D. F. P.; Zhang, X. *Nat. Photon.* **2008**, 10.1038/nphoton.2008.131.
(13) Danckwerts, M.; Novotny, L. *Phys. Rev. Lett.* **2007**, *98*, 026104.
(14) Xu, H.; Bjerneld, E. J.; Käll, M.; Börjesson, L. *Phys. Rev. Lett.* **1999**, *83*, 4357–4360.
(15) Gonzalez, M. U.; Weeber, J. C.; Baudrion, A. L.; Dereux, A.; Stepanov, A. L.; Krenn, J. R.; Devaux, E.; Ebbesen, T. W. *Phys. Rev. B* **2006**, *73*, 155416.
(16) Liz-Marzán, L. M. *Langmuir* **2006**, *22*, 32–41.
(17) Miyazaki, H. T.; Kurokawa, Y. *Phys. Rev. Lett.* **2006**, *96*, 097401.

(18) Conway, J. A.; Sahni, S.; Szkopek, T. *Opt. Express* **2007**, *15*, 4474–4484.
(19) (a) García de Abajo, F. J.; Howie, A *Phys. Rev. Lett.* **1998**, *80*, 5180–5183. (b) García de Abajo, F. J.; Howie, A *Phys. Rev. B* **2002**, *65*, 115418.
(20) García de Abajo, F. J.; Pattantyus-Abraham, A. G.; Zabala, N.; Rivacoba, A.; Wolf, M. O.; Echenique, P. M *Phys. Rev. Lett.* **2003**, *91*, 143902.
(21) Johnson, P. B.; Christy, R. W. *Phys. Rev. B* **1972**, *6*, 4370–4379.
(22) Palik, E. D. *Handbook of Optical Constants of Solids*; Academic Press: New York, 1985.
(23) Fussell, D. P.; McPhedran, R. C.; Martijn de Sterke, C. *Phys. Rev. E* **2004**, *70*, 066608.
(24) Blanco, L. A.; García de Abajo, F. J. *Phys. Rev. B* **2004**, *69*, 205414.
(25) Romero, I.; Aizpurua, J.; Bryant, G. W.; García de Abajo, F. J *Opt. Express* **2006**, *14*, 9988–9999.
(26) Nordlander, P.; Oubre, C.; Prodan, E.; Li, K.; Stockman, M. I. *Nano Lett.* **2004**, *4*, 899–903.
(27) Ashley, J. C.; Emerson, L. C. *Surf. Sci.* **1974**, *41*, 615–618.
(28) Webb, K. J.; Li, J. *Phys. Rev. B* **2005**, *72*, 201402(R)..
(29) Ashcroft, N. W.; Mermin, N. D. *Solid State Physics*; Harcourt College Publishers: New York, 1976.

NL802044T